

# 1 Multi-omics highlights ABO plasma protein as a 2 causal risk factor for COVID-19

3 Ana I. Hernández Cordero<sup>1</sup>, Xuan Li<sup>1</sup>, Stephen Milne<sup>1,2,3</sup>, Chen Xi Yang<sup>1</sup>, Yohan Bossé<sup>4</sup>,  
4 Philippe Joubert<sup>4</sup>, Wim Timens<sup>5</sup>, Maarten van den Berge<sup>6</sup>, David Nickle<sup>7</sup>, Ke Hao<sup>8</sup>, Don D.  
5 Sin<sup>1,2</sup>

6  
7 <sup>1</sup>Centre for Heart Lung Innovation, University of British Columbia, Vancouver, BC, Canada

8  
9 <sup>2</sup> Division of Respiratory Medicine, Faculty of Medicine, University of British Columbia,  
10 Vancouver, BC, Canada

11  
12 <sup>3</sup> Faculty of Medicine and Health, University of Sydney, Sydney, New South Wales,  
13 Australia

14  
15 <sup>4</sup> Institut universitaire de cardiologie et de pneumologie de Québec - Université Laval,  
16 Québec City, QC, Canada

17  
18 <sup>5</sup> University of Groningen, University Medical Centre Groningen, Department of Pathology  
19 and Medical Biology, Groningen, The Netherlands

20  
21 <sup>6</sup> University of Groningen, University Medical Center Groningen, Department of Pulmonary  
22 Diseases, Groningen, The Netherlands

23  
24 <sup>7</sup> Merck Research Laboratories, Genetics and Pharmacogenomics, Boston, Massachusetts,  
25 United States of America

26  
27 <sup>8</sup> Department of Genetics and Genomic Sciences and Icahn Institute for Data Science and  
28 Genomic Technology, Icahn School of Medicine at Mount Sinai, New York, NY, United  
29 States of America

30  
31 **Corresponding author:** Ana I. Hernández Cordero, PhD

32 **Email:** Ana.Hernandez@ubc.hli.ca

33 **Address:** Centre for Heart Lung Innovation, Room 164,  
34 1081 Burrard Street, St. Paul's Hospital, Vancouver, BC V6Z 1Y6

35  
36

37

38

39

40 **Abstract**

41  
42 SARS-CoV-2 is responsible for the coronavirus disease 2019 (COVID-19) and the current  
43 health crisis. Despite intensive research efforts, the genes and pathways that contribute to  
44 COVID-19 remain poorly understood. We therefore used an integrative genomics (IG)  
45 approach to identify candidate genes responsible for COVID-19 and its severity. We used  
46 Bayesian colocalization (COLOC) and summary-based Mendelian randomization to  
47 combine gene expression quantitative trait loci (eQTLs) from the Lung eQTL (n=1,038) and  
48 eQTLGen (n=31,784) studies with published COVID-19 genome-wide association study  
49 (GWAS) data from the COVID-19 Host Genetics Initiative. Additionally, we used COLOC to  
50 integrate plasma protein quantitative trait loci (pQTL) from the INTERVAL study (n=3,301)  
51 with COVID-19-associated loci. Finally, we determined any causal associations between  
52 plasma proteins and COVID-19 using multi-variable two-sample Mendelian randomization  
53 (MR). We found that the expression of 20 genes in lung and 31 genes in blood was  
54 associated with COVID-19. Of these genes, only three (*LZTFL1*, *SLC6A20* and *ABO*) had  
55 been previously linked with COVID-19 in GWAS. The novel loci included genes involved in  
56 interferon pathways (*IL10RB*, *IFNAR2* and *OAS1*). Plasma ABO protein, which is  
57 associated with blood type in humans, demonstrated a significant causal relationship with  
58 COVID-19 in MR analysis; increased plasma levels were associated with an increased risk  
59 of having COVID-19 and risk of severe COVID-19. In summary, our study identified genes  
60 associated with COVID-19 that may be prioritized for future investigation. Importantly, this is  
61 the first study to demonstrate a causal association between plasma ABO protein and  
62 COVID-19.

63  
64 **Key words:** COVID-19, ABO, genomics, proteomics

## 65 **Declarations**

### 66 ***Funding***

67 A.I.H.C. and S.M. are funded by MITACS Accelerate grant. D.D.S. holds the De Lazzari  
68 Family Chair at HLI and a Tier 1 Canada Research Chair in COPD. Y.B. holds a Canada  
69 Research Chair in Genomics of Heart and Lung Diseases.

70

### 71 ***Competing interests***

72 S.M. reports personal fees from Novartis and Boehringer-Ingelheim, outside the submitted  
73 work. W.T. reports fees to Institution from Roche-Ventana, AbbVie, Merck-Sharp-Dohme  
74 and Bristol-Myers-Squibb, outside the submitted work. M.v.d.B. reports research grants  
75 paid to Institution from Astra Zeneca, Novartis, outside the submitted work. D.D.S. reports  
76 research funding from AstraZeneca and received honoraria for speaking engagements from  
77 Boehringer Ingelheim and AstraZeneca over the past 36 months, outside of the submitted  
78 work.

79

### 80 ***Ethics approval and consent to participate***

81 Not applicable

82

### 83 ***Consent to participate***

84 Not applicable

85

### 86 ***Consent for publication***

87 Not applicable

88

### 89 ***Availability of data and materials***

90 The results associated to this manuscript are available on the additional file. Specific  
91 datasets used to conduct this research are available as follow: The COVID-19 summary  
92 statistic can be accessed through the COVID-19 HG website (<https://www.covid19hg.org/>).  
93 Lung eQTL study expression and genotype data can be obtained through GEO platform  
94 accession number GSE23546 and the dbGaP Study Accession phs001745.v1.p1,  
95 respectively. Blood cis-eQTLs summary statistics can be accessed through the eQTLGen  
96 website (<https://www.eqtlgen.org/cis-eqtls.html>). The INTERVAL study pQTLs summary  
97 statistic are available through the European Genotype Archive (accession number  
98 EGAS00001002555).

99

### 100 ***Code availability***

101 Not applicable

102

### 103 ***Authors' contributions***

104 DDS and AIHC designed the study. XL and AIHC conducted the data analyses. AIHC wrote  
105 the first draft of the manuscript. SM was involved in the interpretation of the results and  
106 critical review of the manuscript. CXY revised the manuscript. YB, PJ, WT, MB, DN, KH  
107 provided the lung cis-eQTLs dataset and revised the manuscript. DDS supervised this  
108 study, contributed to the interpretation of the results and revised the manuscript. All authors  
109 read and approved the final manuscript.

110 **Acknowledgments**

111 The eQTL data from Laval University were generated from tissues obtained through the  
112 Quebec Research Respiratory Network Biobank, IUCPQ site. We acknowledge Compute  
113 Canada, which provided computational resources to conduct this research.

114

115

116

117

118

119

120

121

122

123

124

125

126

127

128

129

130

131

132

133

134

135

136 **Introduction**

137

138 The severe acute respiratory syndrome coronavirus 2 (SARS-CoV-2) is responsible for the  
139 coronavirus disease 2019 (COVID-19) and the current world pandemic. The SARS-CoV-2  
140 was first identified in Wuhan, Hubei province, China in late 2019 and since then, it has  
141 spread across the world, affecting more than 180 countries (Zhu et al. 2020). To date, the  
142 COVID-19 health crisis has resulted in the loss of 973,443 human lives (Dong et al. 2020).  
143 While the disease has mild effects in most individuals, severe COVID-19 is more likely in  
144 the elderly population and individuals with comorbidities such as cardiovascular diseases  
145 and diabetes (Zhou et al. 2020a). Why these populations are at a higher risk of adverse  
146 COVID-19 outcomes is still unclear.

147

148 Genetic variations in the host may explain some of the heterogeneity in COVID-19  
149 outcomes. Understanding the role of genetic variants may also provide critical insights into  
150 COVID-19 pathogenesis. However, the genes and pathways that contribute to SARS-CoV-  
151 2 infection are poorly understood. Recently, a pooled genome-wide association study  
152 (GWAS) revealed novel susceptibility loci, including 3p21.31 and 9q34.2, for severe  
153 COVID-19 related to respiratory failure (Ellinghaus et al. 2020). These loci encompassed  
154 several genes, but which (if any) of the individual genes are causally associated with  
155 COVID-19 was not explored.

156

157 GWAS leverages genetic variants to determine associations between regions of the  
158 genome and a particular trait (e.g. disease). However, traditional GWAS has several  
159 limitations that may prevent true gene-trait associations from being identified. For example,  
160 due to correction for multiple comparisons, GWAS results necessarily have a stringent

161 threshold for statistical significance and relevant associations below this threshold may be  
162 missed. Second, disease-associated loci are typically thousands of base pairs wide and  
163 thus contain multiple genes, which may obscure the causal gene contributing to the disease  
164 trait. One emerging approach to identify genes within susceptibility loci is integrative  
165 genomics. By combining genomic information with transcriptomic, proteomic and/or  
166 methylation data, integrative genomics is able to fine-map genetic susceptibility loci and  
167 identify genes and proteins most likely to have a causal association with disease. This  
168 method has previously elucidated specific protein coding genes and mechanisms that  
169 contribute to complex traits (Cano-Gamez and Trynka 2020). In the present study, we  
170 harnessed the power of integrative genomics to identify several susceptibility genes for  
171 COVID-19 and investigate the causal relationship between the plasma protein levels of  
172 candidate genes and COVID-19. Notably, here, we demonstrate a causal association of the  
173 ABO protein (this protein is responsible for the ABO blood groups) with both the risk for  
174 COVID-19 and its severity.

175

## 176 **Methods**

177

### 178 ***Study cohorts***

179

#### 180 *COVID-19 Host Genetics Initiative (COVID-19 HG)*

181 For our study we obtained publicly available summary statistics from the COVID-19 HG  
182 GWAS meta-analysis V3 (<https://www.covid19hg.org/>) (The COVID-19 Host Genetics  
183 Initiative 2020). We obtained the summary statistics for two case-control analyses: 1)  
184 "susceptibility to COVID-19" (where cases were all individuals with a diagnosis of COVID-

185 19 [n=6,696], and controls were all individuals without a COVID-19 diagnosis  
186 [n=1,073,072]; and 2) “Severe COVID-19” (where cases were individuals with a COVID-19  
187 diagnosis and who were hospitalized [n = 3,199], and controls were all individuals without a  
188 COVID-19 diagnosis and no hospitalization [n = 897,488]). In brief, the COVID-19 HG is an  
189 ongoing initiative that aims to shared resources and facilitate COVID-19 genetic host  
190 research through international collaboration. Contributing investigators submit individual  
191 level data or summary results from GWASs performed according to pre-specified  
192 methodological standards to ensure quality and consistency of the data. For imputation  
193 each individual study used their own reference panel or existing imputation panel; the  
194 association analyses were adjusted for age, sex and population structure. The COVID-19  
195 HG combines this data in an inverse variance weighted meta-analysis using variants with  
196 minor allele frequency (MAF) > 0.0001 and imputation quality ( $r^2$ ) > 0.6. Further details are  
197 provided by the COVID-19 HG (The COVID-19 Host Genetics Initiative 2020).

#### 198 *Lung eQTL study*

199 For our study we obtained lung expression quantitative loci (eQTL) from the eQTL study. In  
200 summary, the lung eQTL study cohort consisted of 1,038 participants from three  
201 institutions, University of British Columbia (UBC), Laval University and University of  
202 Groningen. At UBC and Laval University the studies were approved by the ethics  
203 committees within each institution. For University of Groningen the lung specimens were  
204 provided by the local tissue bank of the Department of Pathology, the study protocol used  
205 was consistent with the Research Code of the University Medical Center Groningen and  
206 Dutch national ethical and professional guidelines (“Code of conduct; Dutch federation of  
207 biomedical scientific societies”, <http://www.federa.org>). This study determined the gene  
208 expression of non-tumour lung tissue samples using 43,466 non-control probe sets (see  
209 GEO platform GPL10379). The participants were also genotyped using the Illumina Human

210 1M Duo BeadChip, and after imputation a total of 7,640,142 single nucleotide  
211 polymorphisms (SNPs) for Laval, 7,610,179 for UBC, and 7,741,505 for Groningen were  
212 kept for an eQTL analysis. Data for each site were evaluated, separately, using a linear  
213 regression model, which assumed an additive genotype effect. Site-specific results were  
214 then combined by meta-analysis using a fixed effects model with inverse variance  
215 weighting. cis expression quantitative trait loci (cis-eQTLs) were defined by a 2 Mb window  
216 ( $\pm$  1Mb probe to SNP distance). Full details of the cohort and genotyping quality control,  
217 and eQTL analysis are provided by Hao and colleagues (Hao et al. 2012).

#### 218 *eQTLGen*

219 We obtained blood cis-eQTL summary statistics from eQTLGen. The eQTLGen cohort used  
220 to estimate the cis-eQTLs consisted of 31,684 whole blood (85%) and peripheral blood  
221 mononuclear cell (15%) samples from 37 datasets. Gene expression profiles and  
222 genotypes were obtained for the eQTLGen cohort. The full details on the participants, gene  
223 expression processing and genotyping for each dataset are described by the eQTLGen  
224 consortium (Võsa et al. 2018). The cis-eQTL analysis was performed in each separate  
225 dataset and were estimated within a 2 Mb window ( $\pm$  1Mb probe to SNP distance) as  
226 previously described by Westra and colleagues (Westra et al. 2013), later the results were  
227 combine by meta-analysis using a weighted Z-score method (Westra et al. 2013; Võsa et  
228 al. 2018).

#### 229 *INTERVAL study*

230 We used plasma protein quantitative trait loci (pQTL) obtained from the INTERVAL study  
231 (Sun et al. 2018). In brief, the INTERVAL study was a randomized trial of blood donation  
232 intervals that comprises around 50,000 participants from 25 static donor centres of NHS  
233 Blood and Transplant (NHSBT) (Di Angelantonio et al. 2017; Sun et al. 2018). Blood was  
234 collected from the participants using standard venepuncture. The Affymetrix Axiom UK

235 Biobank array was used for the genotyping of 830,000 SNPs and genotypes were later  
236 imputed using the 1000 Genome phase 3 UK10K reference panel. After quality controls  
237 10,572,788 SNPs were retained. A randomly-selected subset of 3,301 participants were  
238 used for the plasma pQTL analyses of 3,622 proteins (Sun et al. 2018). Plasma protein  
239 levels were measured by using an expanded version of an aptamer-based multiplex protein  
240 assay (SOMAscan) previously described by Sun and colleagues (Sun et al. 2018). The  
241 protein levels were adjusted for confounding variables (age, sex, waiting period between  
242 blood collection and processing and the first three genetic principal components) and the  
243 residuals were extracted and rank-inverse normalized. pQTL analysis consisted of testing  
244 genetic associations with a linear regression using an additive genetic model. The results  
245 from each donor centers were combined using fixed-effect inverse-variance meta-analysis.  
246 Further details on the study cohort, genotyping protocol and quality control are described by  
247 Sun and colleagues (Sun et al. 2018).

248

## 249 ***Integrative-omics methods***

250

### 251 *Bayesian Colocalization test (Coloc)*

252 We first conducted Coloc tests to determine the probability that SNPs associated to COVID-  
253 19 phenotypes and gene expression (eQTLs) were consistent with shared genetic causal  
254 variants (colocalization). This integrative genomic method estimates the ‘posterior  
255 probabilities’ (PP) of five hypothesis described as follow: a genetic locus has no  
256 associations with either of the two traits (i.e. gene expression and a complex trait)  
257 investigated ( $H_0$ ); the locus is associated only with gene expression ( $H_1$ ); the locus is  
258 associated only with the complex trait ( $H_2$ ); the locus is associated with both traits via  
259 independent SNPs ( $H_3$ ); the locus is associated with both traits through shared SNPs ( $H_4$ )

260 (i.e.: a SNP is associated with COVID-19 and is also a cis-eQTL). Colocalization is  
261 therefore indicated by a high PP of  $H_4$  being true. For these analyses we used the coloc  
262 package(Giambartolomei et al. 2014) implemented in R. We tested only cis-eQTL regions  
263 ( $\pm$  1Mb probe to SNP distance). As required by the method and recommended by  
264 Giambartolomei and colleagues (Giambartolomei et al. 2014) we set ‘prior probability’ of the  
265 various configurations ( $H_1$ ,  $H_2$ , and  $H_4$ ). For the eQTL dataset we used  $1 \times 10^{-04}$  prior  
266 probability for a cis-eQTL ( $H_1$ ). We also used  $1 \times 10^{-04}$  prior probability for COVID-19  
267 associations ( $H_2$ ). Finally, we set a prior probability that a single variant affects both traits  
268 ( $H_4$ ) to be  $1 \times 10^{-06}$ . We set significant colocalization (posterior probability) at  $PP_{H_4} > 0.80$ .  
269 We executed coloc between the loci associated to COVID-19 (susceptibility and disease  
270 severity) and cis-eQTLs associated to gene expression in both lung and blood tissues,  
271 retaining genes whose expression colocalized with COVID-19 in both compartments as  
272 ‘candidate genes’. If the corresponding proteins of the candidate genes were present in the  
273 plasma protein dataset (INTERVAL study) we executed Coloc analysis for the plasma  
274 protein levels and COVID-19 phenotypes.

#### 275 *Summary-based Mendelian Randomization (SMR)*

276 The SMR method was specifically built to test the association between gene expression  
277 and a complex trait using a SNP as the instrument (Zhu et al. 2016). SMR is based on the  
278 standard Mendelian Randomization (MR) analysis, where the effect of genetic variants are  
279 linked to the trait of interest via an exposure (gene expression) (Swerdlow et al. 2016).  
280 Therefore, we employed SMR method to identify genes whose expression in lung and  
281 blood may mediate the effect of genetic variants on COVID-19. For the SMR the lung and  
282 blood cis-eQTLs and COVID-19 HG GWAS meta-analysis summary statistics were used.  
283 We selected the 1000G phase 3 EUR (1000 Genomes Project Consortium et al. 2015) as  
284 the reference panel for linkage disequilibrium (LD) estimation. Significant SMR was defined

285 at  $P_{SMR} < 0.001$ . The significant SMR by itself does not necessarily means that the same  
286 variants are associated with the gene expression and the phenotype; the association could  
287 be a consequence of the LD between independent causal variants, rather than pleiotropy of  
288 a single causal variant or causality. To determine whether the associations were related to  
289 LD we used the heterogeneity in dependent instruments test (HEIDI) test (Zhu et al. 2016),  
290 the null hypothesis of which is that the effect of a variant is shared for gene expression and  
291 the phenotype; rejecting the null hypothesis based on the p value ( $P_{HEIDI}$ ) is interpreted as  
292 evidence of heterogeneity (linkage) (Zhu et al. 2016). We reported the significant SMR  
293 associations that also show  $P_{HEIDI} > 0.05$ .

#### 294 *Mendelian Randomization: ABO plasma protein and COVID-1-9*

295 To test causality of the ABO plasma protein we conducted MR tests of the plasma protein  
296 on COVID-19 phenotypes. MR is based on the unidirectional flow of genetic information,  
297 which assumes that genetic variants will have an effect on downstream phenotypes (gene  
298 → protein → phenotype). MR uses SNPs as instrumental variables (IVs) to link a risk factor  
299 ('exposure') to a health trait ('outcome'). The MR assumptions are as follow: IVs are  
300 associated with the exposure, and only affect an outcome *via* the exposure, and are  
301 independent of confounders.

302 A pQTL on chromosome 9q34.2 was identified for ABO plasma protein (Sun et al. 2018).  
303 We performed stepwise conditional analysis, using GCTA 1.92.0beta3 (Yang et al. 2011),  
304 within each 2 Mb region on chromosome 9 to identify independently associated SNPs. UK  
305 Biobank genotypes (Bycroft et al. 2018) were used as the reference sample, and excluded  
306 SNPs with MAF < 0.01. We later extracted the effect size (beta) and standard error (SE) for  
307 each independent variant. Likewise, we obtained the beta and SE for each of these SNPs  
308 on the two COVID-19 phenotypes in the COVID-19 HG meta-analysis. We then performed  
309 an inverse variance weighted (IVW) MR (IVW-MR) (implemented in

310 'MendelianRandomization' R package (Staley 2020)) to link the allelic effects on the  
311 exposure (plasma protein levels) to their effects on the outcome (severe COVID-19 and  
312 COVID-19 diagnosis). We adjusted for possible correlations between SNPs by  
313 incorporating the estimated LD on 1000G phase 3 EUR using PLINK 1.9 (Chang et al.  
314 2015) into MR input. The IVW-MR assumes no directional pleiotropy (i.e. genetic variant  
315 associated with multiple unrelated phenotypes) (Bowden et al. 2015). Significance of the  
316 MR estimate was set at  $P < 0.05$ . To assess the presence of pleiotropy we then executed  
317 MR-Egger analysis (Bowden et al. 2015) which, unlike IVW-MR, allows the estimation of  
318 directional pleiotropy. The presence of pleiotropy is suggested by a significant ( $P_{Egger\ Intercept}$   
319  $< 0.05$ ), non-zero, intercept term.

320 We assessed heterogeneity of the IVs using the Cochran's Q test obtained from the IVW-  
321 MR output (Staley 2020); significant heterogeneity ( $P < 0.05$ ) suggests that the variability of  
322 the IVs estimates is greater than would be expected by chance alone, which may indicate  
323 bias due to invalid IVs. Although a MR with multiple IVs has greater power compared to a  
324 single IV MR, it is possible that the average causal effect may be mainly driven by the SNP  
325 with the strongest association with the outcome. To evaluate the reliance of the multi-  
326 variable MR on individual SNPs we performed a sensitivity analysis by excluding each SNP  
327 at a time and re-calculating the IVW-MR estimate. If removing a SNP significantly changes  
328 the MR estimate, it indicates that the multi-variable MR relied mostly on the removed SNP.

329

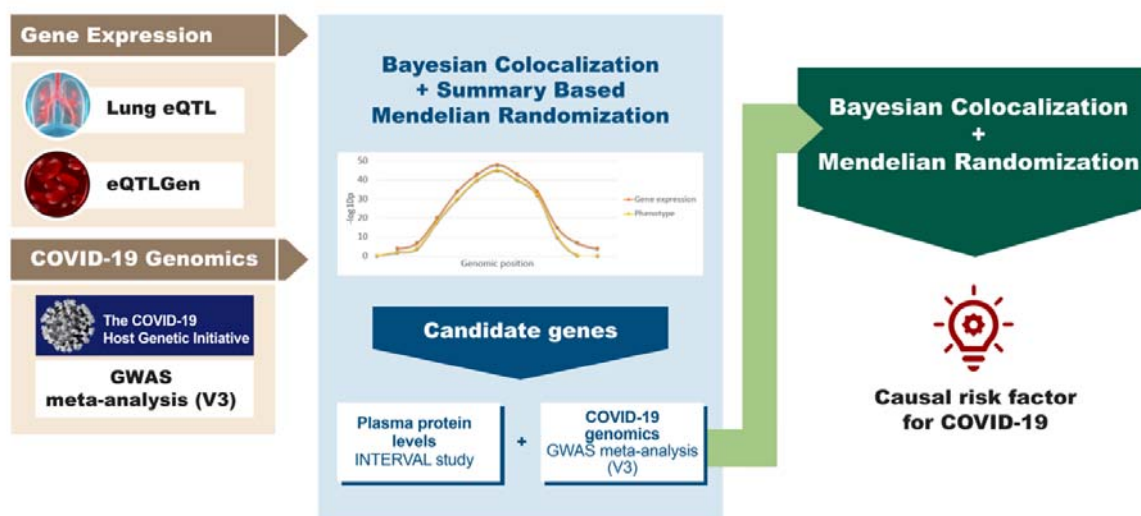
## 330 **Results**

331

### 332 ***Integration of gene expression and COVID-19 genomics reveals novel gene*** 333 ***associations***

334

335 The COVID-19 HG GWAS identified one genetic locus associated with susceptibility to  
336 COVID-19 (defined as a positive COVID-19 diagnosis versus the general population) and  
337 one genetic locus associated with severe COVID-19 (defined as hospitalization for COVID-  
338 19 versus the general population) at a genome-wide significant threshold of  $P_{GWAS} < 5 \times 10^{-8}$ .  
339 In our analysis, in addition to these loci, we also explored regions below this stringent  
340 threshold. We integrated these GWAS results with gene expression data from both lung  
341 tissue (Lung eQTL Study) and blood (eQTLGen) using two statistical methodologies  
342 (described in detail in the Methods) (**Fig. 1**). Bayesian colocalization assess whether two  
343 genetic association signals are consistent with a shared causal variant. We defined  
344 colocalization as the posterior probability of this hypothesis ( $PP_{H4}$ ) being  $> 0.80$ . SMR  
345 integrates summary data from GWAS and eQTLs in order to identify genes whose  
346 expression levels are associated with a trait due to the effects of a common genetic variant  
347 (either by direct causal or pleiotropic effects) rather than due to genetic linkage.  
348 Significance of SMR estimate was set at  $P_{SMR} < 0.001$  with no significant heterogeneity  
349 ( $P_{HEIDI} > 0.05$ ).  
350



351

352 **Fig. 1 Study overview.** The diagram summarizes the genomics datasets and analytic  
353 pipeline of the study. First, publicly available -omics datasets were obtained, which were  
354 later processed using integrative genomics (IG) methods (Bayesian Colocalization and  
355 Summary-based Mendelian Randomization) to identify potential candidate genes for  
356 COVID-19 phenotypes. Lastly, using a Bayesian Colocalization and Mendelian  
357 Randomization approach we explored the causal association between the plasma protein  
358 levels of the most promising candidate gene and COVID-19.  
359

#### 360 *Lung gene expression*

361 The expression of 14 unique genes in lung tissue co-localized ( $PP_{H4}$  being  $> 0.80$ ) with  
362 severe COVID-19 associated loci (**Fig. 2a**) and 3 with the COVID-19 diagnosis associated  
363 loci (**Supplementary Table S1**). The majority of the gene associations identified in lung  
364 tissue were novel (i.e. not been identified by previous GWAS), and in most cases (10 out of  
365 14), the genes met the suggestive statistical significance ( $P_{GWAS} < 5 \times 10^{-05}$ ) rather than the  
366 genome-wide significance ( $P_{GWAS} < 5 \times 10^{-08}$ ) (**Supplementary Table S1**). For example:  
367 *IL10RB* and *IFNAR2* (**Fig. 2a**) are interferon (IFN) receptor genes that co-localized with  
368 COVID-19 ( $PP_{H4} > 0.80$ ); these genes were located in the same suggestive locus on  
369 chromosome 21 (sentinel SNP rs9976829,  $P_{GWAS} = 7.2 \times 10^{-07}$  [COVID-19 hospitalization  
370 vs population] (The COVID-19 Host Genetics Initiative 2020)). In addition, results from the  
371 SMR show that the increased expression of *IFNAR2* in lung tissue was associated with  
372 decreased the risk of severe COVID-19 (**Supplementary Table S2**) and susceptibility to  
373 COVID-19 (**Fig. 2b**) ( $P_{SMR} < 0.001$ ). SMR also identified a first-time association for the gene  
374 *OAS1* (**Fig. 2b and Supplementary Table S2**), which is an interferon stimulated gene  
375 involved in the cellular response to viral infection; increased expression of this gene was  
376 associated with decreased susceptibility to COVID-19.

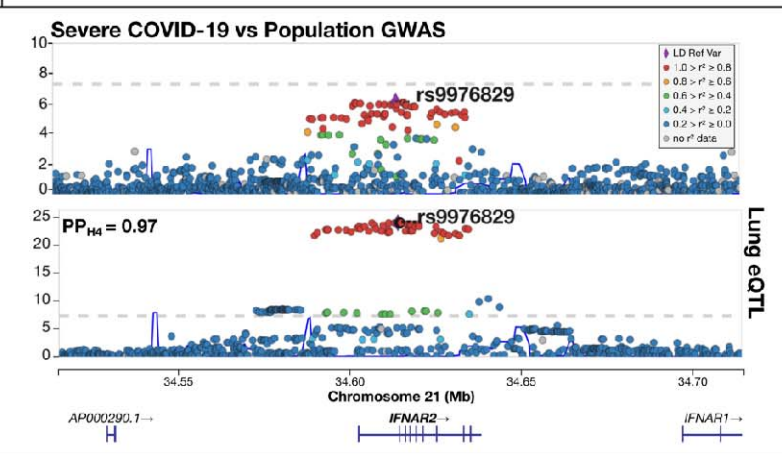
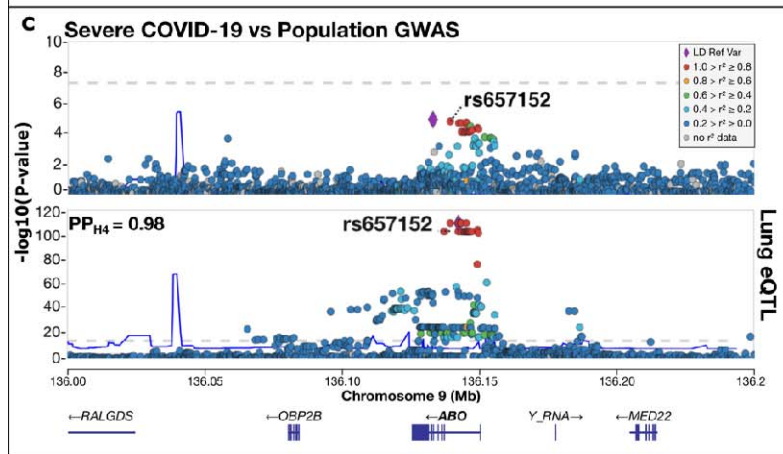
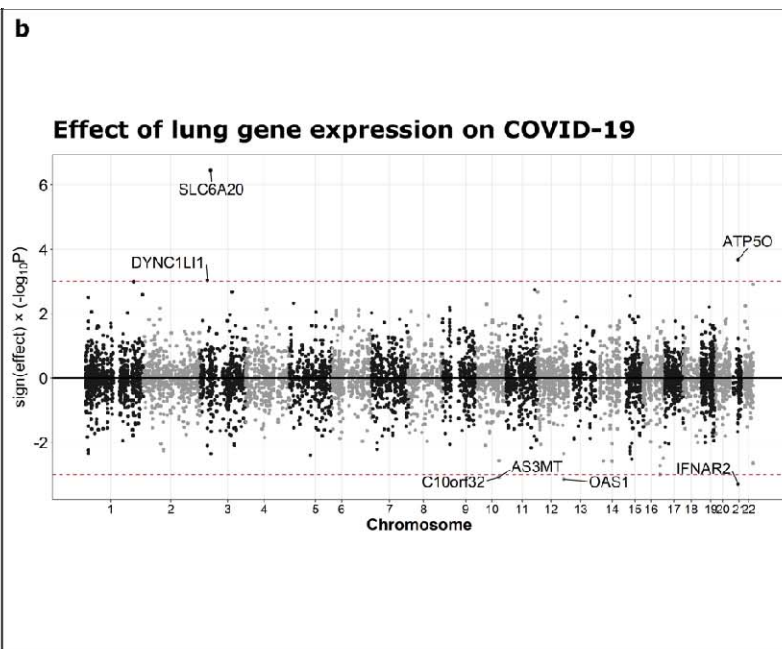
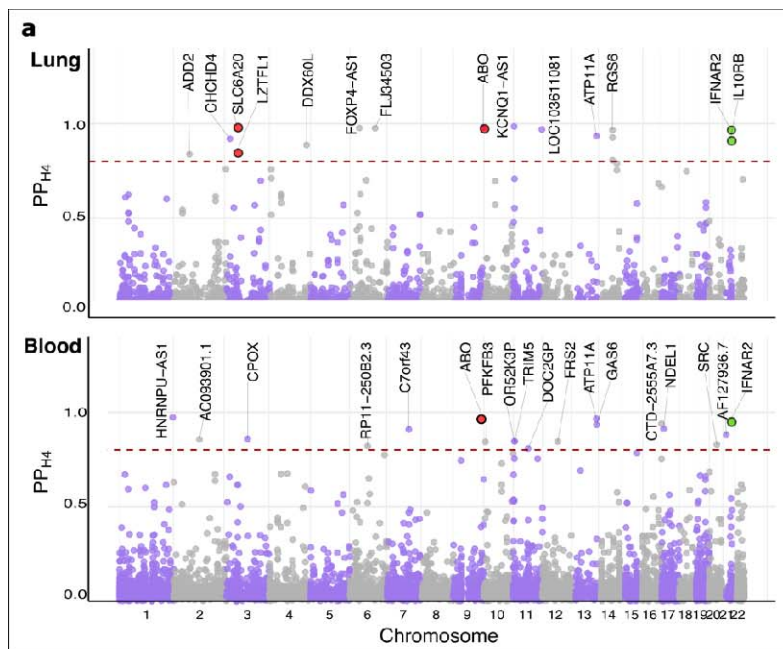
377

378 In addition to these novel gene associations, three co-localized genes (*LZTFL1*, *SLC6A20*  
379 and *ABO*) were within loci that have been previously associated with severe COVID-19 by

380 GWAS(Ellinghaus et al. 2020) (**Fig. 2a**). SMR showed that increased *SLC6A20* expression  
381 in lung tissue was associated with increased the risk of severe COVID-19 (**Supplementary**  
382 **Table S2**) and susceptibility to COVID-19 (**Fig. 2b**). *ABO* gene expression co-localized with  
383 severe COVID-19 **Fig. 2c**. The colocalization between *ABO* gene expression and the  
384 COVID-19 susceptibility associated loci was not tested since the variants associated with  
385 this gene in the lung eQTL and eQTLGEN studies were not present in the COVID-19 HG  
386 meta-analysis for this phenotype.

### 387 *Blood gene expression*

388 In blood, the expression of 18 and 8 unique genes co-localized with COVID-19 severity  
389 (**Fig. 2a**) and susceptibility associated loci (**Supplementary Table S1**), respectively. The  
390 expression of *ABO* in blood co-localized with severe COVID-19 associated loci. In addition,  
391 *IFNAR2* expression in blood co-localized with both COVID-19 phenotypes, although its  
392 strongest colocalization ( $PP_{H4} = 0.96$ ) was found with the COVID-19 hospitalization  
393 phenotype. Other first-time associations within COVID-19 suggestive loci included  
394 *HNRNPU-AS1*, *ATP11A* and *CTD-2555A7.3*. SMR identified 22 genes whose expression in  
395 blood was associated with COVID-19 phenotypes (**Supplementary Table S2**). Increased  
396 blood expression levels of *OAS1* and *CPOX* in blood were associated with decreased  
397 susceptibility to COVID-19 and increased risk of severe COVID-19, respectively.



400 **Fig. 2 COVID-19 genomics and gene expression integration.** a) Colocalization of COVID-19 (hospitalization vs population)  
401 with gene expression in lung and blood tissues, respectively. The circles represent the probability (y-axis) that a gene  
402 colocalizes ( $PP_{H4}$ ) with COVID-19 plotted against its chromosomal position (x-axis). The red dashed horizontal line represents  
403 the threshold of significance ( $PP_{H4} > 0.80$ ). Red and green circles highlight the genes within previously identified COVID-19 loci,  
404 and those involved in the interferon pathways, respectively. b) Results from the Summary Based Mendelian Randomization are  
405 displayed in this mirror Manhattan plot. The circles represent the association between susceptibility to COVID-19 (diagnosis vs  
406 population) and the gene expression (lung) multiplied by the direction of the effect (y-axis) plotted against the genes  
407 chromosomal position (x-axis). The dotted horizontal lines (red) represent the threshold of significance ( $P < 0.001$ ). SMR plot only  
408 shows the results that passed the heterogeneity test (see methods). c) Regional plots for severe COVID-19 (COVID-19  
409 hospitalization vs population) and lung tissue cis-eQTL at the *ABO* (left panel) and *IFNAR2* (right panel) loci. Severe GWAS  
410 signals (top of the panel c) colocalize with the cis-QTL region (bottom of the panel C) at *ABO* (chromosome 9) and *IFNAR2*  
411 (chromosome 21). The circles represent the  $-\log_{10}$  association p values (y-axis) of SNPs plotted against their chromosomal  
412 position (x-axis). The co-localized SNP is shown inside each plot and  $PP_{H4}$  is at the left top corner of the lung eQTL regional  
413 plots. Pairwise linkage disequilibrium ( $r^2$ , calculated from the 1000 Genomes European population) in each region is colored  
414 with respect to the lead GWAS SNP within each region.

415

416 ***ABO plasma protein is a risk factor for COVID-19***

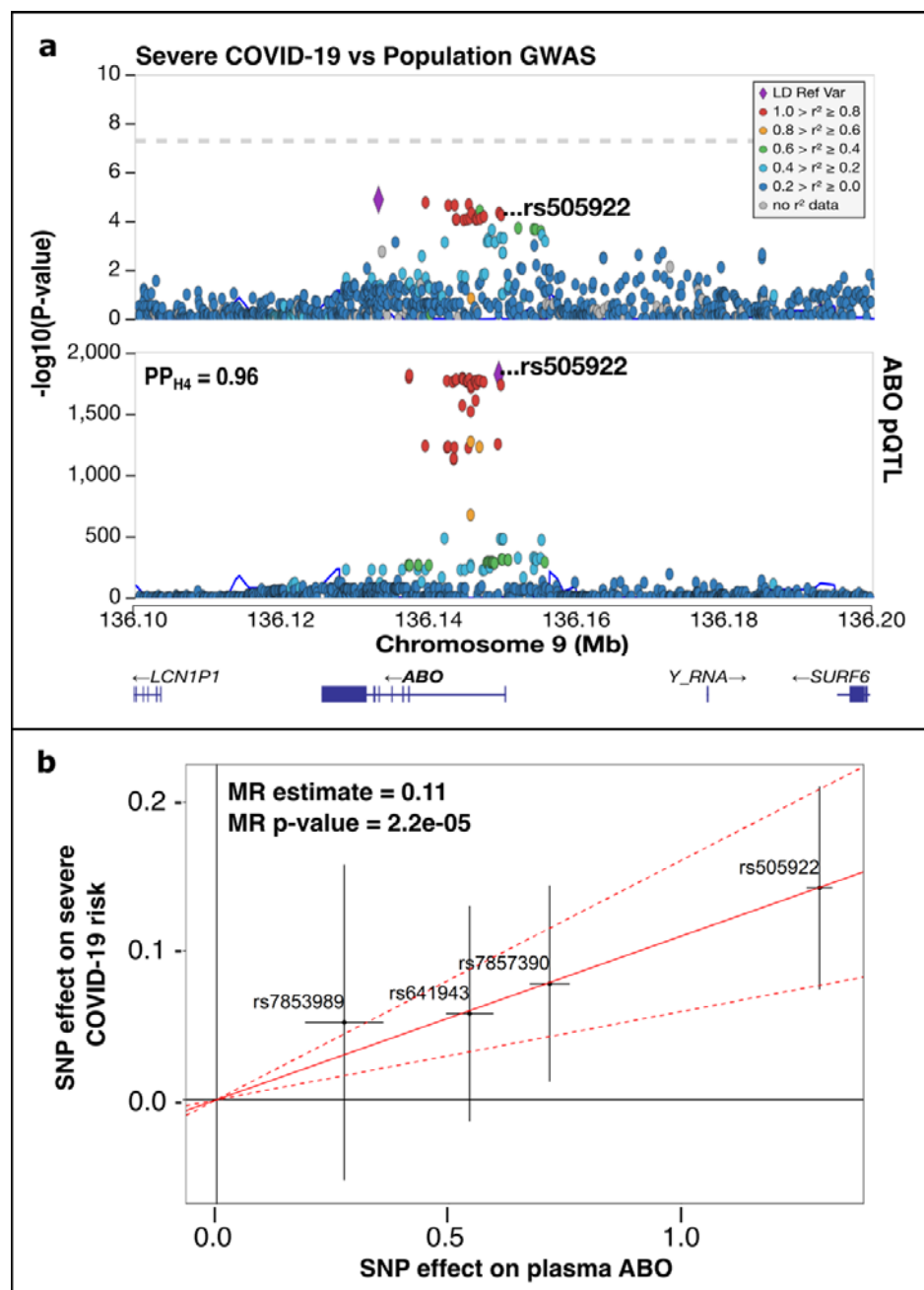
417

418 The functional effects of genes are generally imparted through their translation into  
419 proteins. In order to strengthen the mechanistic association between the identified genes  
420 and COVID-19, we determined which of these genes were associated with both blood  
421 protein levels and COVID-19 phenotypes. We integrated the COVID-19 HG GWAS and  
422 blood protein GWAS from the INTERVAL study (which includes genome-wide associations  
423 between genetic variants and 3,622 blood proteins) using Coloc. Additionally, we applied  
424 MR to determined causal associations between protein and COVID-19.

425

426 Of the three protein-coding candidate genes (*ABO*, *IFNAR2*, and *ATP11A*) whose  
427 expression in both tissues co-localized with COVID-19 phenotypes, only *ABO* was present  
428 in the INTERVAL study. We found that *ABO* plasma protein levels co-localized with  
429 susceptibility to COVID-19 and its severity (**Fig. 3a and Supplementary Table S3**).

430



431

432 **Fig. 3 Bayesian Colocalization (a) and Mendelian Randomization (MR) (b) of ABO**  
 433 **plasma protein and COVID-19.** a) Regional plot describing severe COVID-19 GWAS  
 434 (COVID-19 hospitalization vs population) (top of a) and plasma protein pQTL (bottom of A)  
 435 at the *ABO* locus. The circles represent the  $-\log_{10}$  association p values (y axis) of SNPs  
 436 plotted against their chromosomal position (x-axis). The colocalized SNP is shown inside  
 437 each plot and  $PP_{H4}$  is at the left top corner of the plasma protein pQTL regional plot.  
 438 Pairwise linkage disequilibrium ( $r^2$ , calculated from the 1000 Genomes European  
 439 population) in each region is colored with respect to the lead GWAS SNP within each  
 440 region. b) Inverse variance weighting (IVW) MR (IVW-MR) of ABO plasma proteins on risk  
 441 of severe COVID-19 (COVID-19 hospitalization vs population). The x-axis represents the

442 SNP effect on the plasma protein levels, and the y-axis the SNP effect on severe COVID-  
443 19. The variants used for the MR are shown inside the plot with error bars that represent  
444 the 95% confidence intervals. The slope of the solid red line is the instrumental variables  
445 regression estimate of the effect of the protein on severe COVID-19, with dashed red lines  
446 representing the 95 % confident interval. IVW-MR P-value and estimate are shown in the  
447 top left corner.

448

449 An IVW-MR test was conducted using four independent variants as instrumental variables  
450 (IVs) to investigate the causal relationship between ABO plasma protein and COVID-19.

451 Based on the Cochran's Q and MR-Egger intercept p-values the IV's average effect on  
452 COVID-19 phenotypes did not demonstrate significant heterogeneity or horizontal

453 pleiotropy (**Supplementary Table S4**). The results indicated a significant causal

454 association between ABO plasma protein levels and COVID-19 phenotypes ( $P < 0.05$ ) (**Fig.**

455 **3b and Supplementary Figure S1**). Each ABO-increasing allele increased the odds of

456 COVID-19 by 7% and the odds of severe COVID-19 by 11% (**Fig. 3b**). In addition, we

457 performed a sensitivity analysis to assess if the MR results were driven by a single SNP.

458 **Supplementary Figures S2 and S3** show that the exclusion of any of the IVs used for the

459 MR did not significantly change the overall IVW-MR estimate.

460

## 461 **Discussion**

462

463 Recent GWAS have revealed genetic loci that are significantly associated with COVID-19

464 (The COVID-19 Host Genetics Initiative 2020; Ellinghaus et al. 2020); however, since these

465 loci often harbor multiple genes, the underlying genes or pathways responsible for COVID-

466 19 remain unknown. To address this crucial gap in knowledge, we used integrative genomic

467 methods, which unveiled several novel findings. First, we identified gene associations

468 whose physiology plausibly relates to COVID-19. Second, we linked the effect of genetic

469 variants to the gene expression of previously identified COVID-19 related-genes. Third, we

470 showed that genetically-determined plasma ABO protein level is causally associated with  
471 the risk of severe COVID-19 and its susceptibility.

472

473 Although the chromosome 3p21 region has been previously associated with severe COVID-  
474 19, this locus encompasses six genes, making it hard to identify the precise gene  
475 responsible for the association with COVID-19 (Ellinghaus et al. 2020). We found that two  
476 genes within this locus (*SLC6A20* and *LZTFL1*) co-localized with severe COVID-19. The  
477 *SLC6A20* protein product (sodium- and chloride-dependent transporter XTRP3) is involved  
478 in amino acid transport, with a role in the regulation of thymocyte selection (Simeoni et al.  
479 2005) and negative regulation of T-cell activation (Arndt et al. 2011), suggesting its role in  
480 COVID-19 may be due altered immune responses. This protein may also interact with  
481 angiotensin converting enzyme 2 (ACE2), which is the putative SARS-CoV-2 receptor  
482 (Vuille-dit-Bille et al. 2015; Zhou et al. 2020b). Interestingly, both ACE2 and *SLC6A20* gene  
483 and protein expression increase with age (Meier et al. 2018; Bunyavanich et al. 2020;  
484 Vuille-dit-Bille et al. 2020) with the lowest concentrations noted in children (small intestinal  
485 and nasal epitheliums); although children are susceptible to SARS-CoV-2 infection, they  
486 appear to be at very low risk of developing severe COVID-19 (Jordan et al. 2020).  
487 Consistent with these findings, another recent study has shown that a risk variant  
488 (rs11385942) for *SLC6A20* expression in human lung cells conferred an increased risk for  
489 severe COVID-19 (Ellinghaus et al. 2020, p. 19). *LZTFL1* encodes leucine zipper  
490 transcription factor-like protein 1, a protein involved in intracellular cargo trafficking that is  
491 linked to congenital ciliopathies; the mechanism of its association with COVID-19 is unclear.

492

493 Of the newly described gene associations with susceptibility to COVID-19 and severe  
494 COVID-19, *IL10RB*, *IFNAR2* and *OAS1* are notable given their role in the IFN pathways.

495 The protein products of *IFNAR2* and *IL10RB* are components of the receptor complexes for  
496 type I and III IFNs, respectively, which are critical in the early host responses to a viral  
497 infection. The protein product of *OAS1* (2'-5'-oligoadenylate synthase 1), which is induced  
498 by IFNs, indirectly promotes viral RNA degradation and inhibition of viral replication. Our  
499 findings suggest that increased *IFNAR2* and *OAS1* gene expression decreases the  
500 susceptibility to COVID-19 and severe COVID-19. This is consistent with the concept of IFN  
501 dysregulation in severe COVID-19, in which patients mount a delayed and often blunted  
502 IFN response to the virus (Acharya et al. 2020; Made et al. 2020). Our findings support the  
503 results of a recent clinical trial showing that inhaled IFN-beta decreased the risk of severe  
504 COVID-19 (Balfour 2020).

505

506 Our results also show that a COVID-19 locus was associated with *ABO* gene expression in  
507 lung and blood tissues and plasma protein levels in blood. The *ABO* gene encodes for a  
508 protein responsible for the ABO blood groups. While the A and B allele carriers express  
509 glycosyltransferase activities that convert H antigen into A or B antigen, the O group protein  
510 lacks this enzymatic activity (due to a deletion in the gene [frameshift]). Previous studies  
511 have shown that blood type O individuals demonstrated a lower susceptibility to COVID-19  
512 (Zhao et al. 2020; Zietz and Tatonetti 2020; Ellinghaus et al. 2020), and variants in the *ABO*  
513 have been associated with risk of severe COVID-19 (Ellinghaus et al. 2020). Using two-  
514 sample MR analysis, we showed that the ABO plasma protein is likely a causal risk factor  
515 for susceptibility to COVID-19 and severe COVID-19. The mechanism by which ABO  
516 protein modifies COVID-19 risk is unclear. In SARS-CoV a naturally occurring anti-A  
517 antibodies can inhibit spike protein-mediated cellular entry via the ACE2 receptor (Guillon et  
518 al. 2008) (this is also the putative entry mechanism for SARS-CoV-2), it has been  
519 speculated that this effect may also be found in SARS-CoV-2 (Zhao et al. 2020). Another

520 possible explanation is that the A blood type is associated with an increased risk of  
521 cardiovascular disease (Wu et al. 2008), which is a known risk factors for severe COVID-  
522 19, while those with the O blood type are less likely to develop cardiovascular diseases.  
523 Furthermore, previous reports found an incidence of venous thromboembolism (VTE) of  
524 27% in critically ill COVID-19 patients (Klok et al. 2020, p. 19). ABO blood type has been  
525 previously associated with risk of VTE (Wang et al. 2017); interestingly, the protein-  
526 increasing allele (C) of the top SNP (rs505922) used in the MR tests is also a risk variant  
527 for VTE (Trégouët et al. 2009). Further investigation is needed to understand the  
528 physiological role of ABO in the pathophysiology of COVID-19.

529

530 Our study had several limitations. Firstly, our analyses were limited by the number of  
531 genetic variants that overlapped between the COVID-19 HG meta-analysis and the  
532 datasets that were used for this study. Thus, we could not test some genes that may be of  
533 importance. Secondly, replication of our result in an independent dataset was not possible  
534 due to the lack of COVID-19 GWAS data available at the present time; therefore first-time  
535 associations identified by our analyses should be considered with caution. Lastly, the lung  
536 and blood -omics data used reflect the transcriptomic and proteomic profile under normal  
537 conditions, however it is likely that that these associations may change under stimulation by  
538 viral infection or acute inflammation.

539

## 540 **Conclusions**

541

542 We used a multi-omics approach to identify several candidate genes that may be involved  
543 in the pathogenesis of COVID-19. The analyses presented here linked COVID-19 genomics  
544 to gene expression in lung and blood tissues. This approach revealed specific genes within

545 previously implicated COVID-19 loci, and also identified new genes whose biology is  
546 consistent with COVID-19. Importantly, our analysis suggests that the ABO protein is a  
547 causal risk factor for severe COVID-19 and COVID-19 susceptibility.

548

## 549 **Supplementary files**

550

### 551 ***Supplementary Tables:***

552 Table S1: Genes associated to COVID-19 through colocalization.

553 Table S2: Genes associated to COVID-19 through Summary-based Mendelian  
554 Randomization.

555 Table S3. COVID-19 phenotypes and ABO plasma protein colocalization.

556 Table S4. Inverse variance weighting mendelian randomization (IVW-MR) of ABO plasma  
557 protein and COVID-19.

### 558 ***Supplementary Figures:***

559 Figure S1. Mendelian Randomization of ABO plasma protein and susceptibility to COVID-  
560 19.

561 Figure S2. Mendelian Randomization sensitivity analysis for dependence on individual  
562 instruments (severe COVID-19 and ABO plasma protein).

563 Figure S3. Mendelian Randomization (MR) sensitivity analysis for dependence on individual  
564 instruments (susceptibility of COVID-19 and ABO plasma protein).

565

## 566 **References**

567

568 1000 Genomes Project Consortium, Auton A, Brooks LD, et al (2015) A global reference for  
569 human genetic variation. Nature 526:68–74. <https://doi.org/10.1038/nature15393>

- 570 Acharya D, Liu G, Gack MU (2020) Dysregulation of type I interferon responses in COVID-  
571 19. *Nature Reviews Immunology* 20:397–398. [https://doi.org/10.1038/s41577-020-](https://doi.org/10.1038/s41577-020-0346-x)  
572 0346-x
- 573 Arndt B, Krieger T, Kalinski T, et al (2011) The transmembrane adaptor protein SIT inhibits  
574 TCR-mediated signaling. *PLoS ONE* 6:e23761.  
575 <https://doi.org/10.1371/journal.pone.0023761>
- 576 Balfour H (2020) Inhaled interferon beta therapy shows promise in COVID-19 trial. In:  
577 *European Pharmaceutical Review*.  
578 [https://www.europeanpharmaceuticalreview.com/news/123994/inhaled-interferon-](https://www.europeanpharmaceuticalreview.com/news/123994/inhaled-interferon-beta-therapy-shows-promise-in-covid-19-trial/)  
579 [beta-therapy-shows-promise-in-covid-19-trial/](https://www.europeanpharmaceuticalreview.com/news/123994/inhaled-interferon-beta-therapy-shows-promise-in-covid-19-trial/). Accessed 7 Aug 2020
- 580 Bowden J, Davey Smith G, Burgess S (2015) Mendelian randomization with invalid  
581 instruments: effect estimation and bias detection through Egger regression. *Int J*  
582 *Epidemiol* 44:512–525. <https://doi.org/10.1093/ije/dyv080>
- 583 Bunyavanich S, Do A, Vicencio A (2020) Nasal Gene Expression of Angiotensin-Converting  
584 Enzyme 2 in Children and Adults. *JAMA* 323:2427–2429.  
585 <https://doi.org/10.1001/jama.2020.8707>
- 586 Bycroft C, Freeman C, Petkova D, et al (2018) The UK Biobank resource with deep  
587 phenotyping and genomic data. *Nature* 562:203–209.  
588 <https://doi.org/10.1038/s41586-018-0579-z>
- 589 Cano-Gamez E, Trynka G (2020) From GWAS to Function: Using Functional Genomics to  
590 Identify the Mechanisms Underlying Complex Diseases. *Front Genet* 11:.  
591 <https://doi.org/10.3389/fgene.2020.00424>
- 592 Chang CC, Chow CC, Tellier LC, et al (2015) Second-generation PLINK: rising to the  
593 challenge of larger and richer datasets. *Gigascience* 4:.  
594 <https://doi.org/10.1186/s13742-015-0047-8>
- 595 Di Angelantonio E, Thompson SG, Kaptoge S, et al (2017) Efficiency and safety of varying  
596 the frequency of whole blood donation (INTERVAL): a randomised trial of 45 000  
597 donors. *Lancet* 390:2360–2371. [https://doi.org/10.1016/S0140-6736\(17\)31928-1](https://doi.org/10.1016/S0140-6736(17)31928-1)
- 598 Dong E, Du H, Gardner L (2020) An interactive web-based dashboard to track COVID-19 in  
599 real time. *Lancet Infect Dis* 20:533–534. [https://doi.org/10.1016/S1473-](https://doi.org/10.1016/S1473-3099(20)30120-1)  
600 [3099\(20\)30120-1](https://doi.org/10.1016/S1473-3099(20)30120-1)
- 601 Ellinghaus D, Degenhardt F, Bujanda L, et al (2020) Genomewide Association Study of  
602 Severe Covid-19 with Respiratory Failure. *N Engl J Med*.  
603 <https://doi.org/10.1056/NEJMoa2020283>
- 604 Giambartolomei C, Vukcevic D, Schadt EE, et al (2014) Bayesian Test for Colocalisation  
605 between Pairs of Genetic Association Studies Using Summary Statistics. *PLOS*  
606 *Genetics* 10:e1004383. <https://doi.org/10.1371/journal.pgen.1004383>

- 607 Guillon P, Clément M, Sébille V, et al (2008) Inhibition of the interaction between the SARS-  
608 CoV Spike protein and its cellular receptor by anti-histo-blood group antibodies.  
609 *Glycobiology* 18:1085–1093. <https://doi.org/10.1093/glycob/cwn093>
- 610 Hao K, Bossé Y, Nickle DC, et al (2012) Lung eQTLs to help reveal the molecular  
611 underpinnings of asthma. *PLoS Genet* 8:e1003029.  
612 <https://doi.org/10.1371/journal.pgen.1003029>
- 613 Jordan RE, Adab P, Cheng KK (2020) Covid-19: risk factors for severe disease and death.  
614 *BMJ* 368:. <https://doi.org/10.1136/bmj.m1198>
- 615 Klok FA, Kruip MJHA, van der Meer NJM, et al (2020) Incidence of thrombotic  
616 complications in critically ill ICU patients with COVID-19. *Thromb Res* 191:145–147.  
617 <https://doi.org/10.1016/j.thromres.2020.04.013>
- 618 Made CI van der, Simons A, Schuurs-Hoeijmakers J, et al (2020) Presence of Genetic  
619 Variants Among Young Men With Severe COVID-19. *JAMA*.  
620 <https://doi.org/10.1001/jama.2020.13719>
- 621 Meier C, Camargo SM, Hunziker S, et al (2018) Intestinal IMINO transporter SIT1 is not  
622 expressed in human newborns. *American Journal of Physiology-Gastrointestinal and*  
623 *Liver Physiology* 315:G887–G895. <https://doi.org/10.1152/ajpgi.00318.2017>
- 624 Simeoni L, Posevitz V, Kölsch U, et al (2005) The transmembrane adapter protein SIT  
625 regulates thymic development and peripheral T-cell functions. *Mol Cell Biol* 25:7557–  
626 7568. <https://doi.org/10.1128/MCB.25.17.7557-7568.2005>
- 627 Staley OYJ (2020) MendelianRandomization: Mendelian Randomization Package. Version  
628 0.4.3URL <https://CRAN.R-project.org/package=MendelianRandomization>
- 629 Sun BB, Maranville JC, Peters JE, et al (2018) Genomic atlas of the human plasma  
630 proteome. *Nature* 558:73–79. <https://doi.org/10.1038/s41586-018-0175-2>
- 631 Swerdlow DI, Kuchenbaecker KB, Shah S, et al (2016) Selecting instruments for Mendelian  
632 randomization in the wake of genome-wide association studies. *Int J Epidemiol*  
633 45:1600–1616. <https://doi.org/10.1093/ije/dyw088>
- 634 The COVID-19 Host Genetics Initiative (2020) The COVID-19 Host Genetics Initiative, a  
635 global initiative to elucidate the role of host genetic factors in susceptibility and  
636 severity of the SARS-CoV-2 virus pandemic. *European Journal of Human Genetics*  
637 28:715–718. <https://doi.org/10.1038/s41431-020-0636-6>
- 638 Trégouët D-A, Heath S, Saut N, et al (2009) Common susceptibility alleles are unlikely to  
639 contribute as strongly as the FV and ABO loci to VTE risk: results from a GWAS  
640 approach. *Blood* 113:5298–5303. <https://doi.org/10.1182/blood-2008-11-190389>
- 641 Võsa U, Claringbould A, Westra H-J, et al (2018) Unraveling the polygenic architecture of  
642 complex traits using blood eQTL metaanalysis. *bioRxiv* 447367.  
643 <https://doi.org/10.1101/447367>

- 644 Vuille-dit-Bille RN, Camargo SM, Emmenegger L, et al (2015) Human intestine luminal  
645 ACE2 and amino acid transporter expression increased by ACE-inhibitors. *Amino*  
646 *Acids* 47:693–705. <https://doi.org/10.1007/s00726-014-1889-6>
- 647 Vuille-dit-Bille RN, Liechty KW, Verrey F, Guglielmetti LC (2020) SARS-CoV-2 receptor  
648 ACE2 gene expression in small intestine correlates with age. *Amino Acids*.  
649 <https://doi.org/10.1007/s00726-020-02870-z>
- 650 Wang Z, Dou M, Du X, et al (2017) Influences of ABO blood group, age and gender on  
651 plasma coagulation factor VIII, fibrinogen, von Willebrand factor and ADAMTS13  
652 levels in a Chinese population. *PeerJ* 5:. <https://doi.org/10.7717/peerj.3156>
- 653 Westra H-J, Peters MJ, Esko T, et al (2013) Systematic identification of trans eQTLs as  
654 putative drivers of known disease associations. *Nature Genetics* 45:1238–1243.  
655 <https://doi.org/10.1038/ng.2756>
- 656 Wu O, Bayoumi N, Vickers MA, Clark P (2008) ABO(H) blood groups and vascular disease:  
657 a systematic review and meta-analysis. *J Thromb Haemost* 6:62–69.  
658 <https://doi.org/10.1111/j.1538-7836.2007.02818.x>
- 659 Yang J, Lee SH, Goddard ME, Visscher PM (2011) GCTA: a tool for genome-wide complex  
660 trait analysis. *Am J Hum Genet* 88:76–82. <https://doi.org/10.1016/j.ajhg.2010.11.011>
- 661 Zhao J, Yang Y, Huang H, et al (2020) Relationship between the ABO Blood Group and the  
662 COVID-19 Susceptibility. *medRxiv* 2020.03.11.20031096.  
663 <https://doi.org/10.1101/2020.03.11.20031096>
- 664 Zhou F, Yu T, Du R, et al (2020a) Clinical course and risk factors for mortality of adult  
665 inpatients with COVID-19 in Wuhan, China: a retrospective cohort study. *The Lancet*  
666 395:1054–1062. [https://doi.org/10.1016/S0140-6736\(20\)30566-3](https://doi.org/10.1016/S0140-6736(20)30566-3)
- 667 Zhou P, Yang X-L, Wang X-G, et al (2020b) A pneumonia outbreak associated with a new  
668 coronavirus of probable bat origin. *Nature* 579:270–273.  
669 <https://doi.org/10.1038/s41586-020-2012-7>
- 670 Zhu N, Zhang D, Wang W, et al (2020) A Novel Coronavirus from Patients with Pneumonia  
671 in China, 2019. *New England Journal of Medicine* 382:727–733.  
672 <https://doi.org/10.1056/NEJMoa2001017>
- 673 Zhu Z, Zhang F, Hu H, et al (2016) Integration of summary data from GWAS and eQTL  
674 studies predicts complex trait gene targets. *Nat Genet* 48:481–487.  
675 <https://doi.org/10.1038/ng.3538>
- 676 Zietz M, Tatonetti NP (2020) Testing the association between blood type and COVID-19  
677 infection, intubation, and death. *medRxiv*.  
678 <https://doi.org/10.1101/2020.04.08.20058073>
- 679